

UC Merced

UC Merced Previously Published Works

Title

Experimental and Theoretical Evidence for Nitrogen-Fluorine Halogen Bonding in Silver-Initiated Radical Fluorinations

Permalink

<https://escholarship.org/uc/item/1b10x1vd>

Journal

ACS CATALYSIS, 9(4)

ISSN

2155-5435

Authors

Hua, Alyssa M
Bidwell, Samantha L
Baker, Sarah I
[et al.](#)

Publication Date

2019

DOI

10.1021/acscatal.9b00623

Peer reviewed

Experimental and Theoretical Evidence for Nitrogen–Fluorine Halogen Bonding in Silver-Initiated Radical Fluorinations

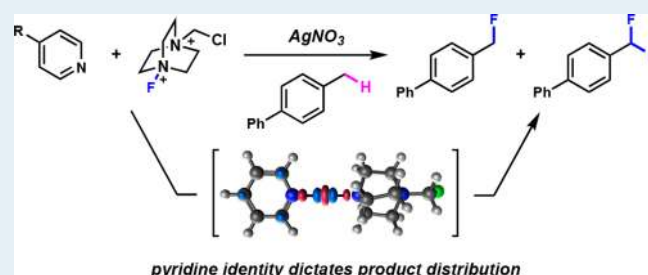
Alyssa M. Hua,^{§,†} Samantha L. Bidwell,^{§,†} Sarah I. Baker,[§] Hrant P. Hratchian,^{*,§,‡} and Ryan D. Baxter^{*,§,‡}

[§]Department of Chemistry and Chemical Biology, University of California, 5200 N. Lake Road, Merced, California 95343, United States

S Supporting Information

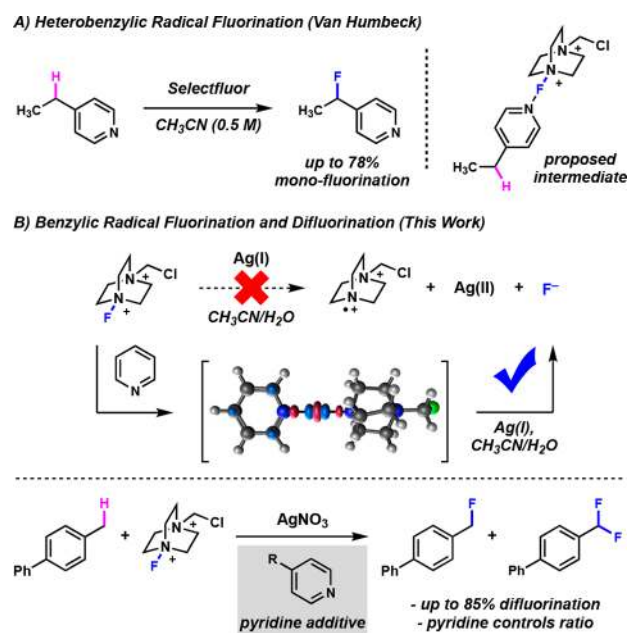
ABSTRACT: We report experimental and computational evidence for nitrogen–fluorine halogen bonding in Ag(I)-initiated radical C–H fluorinations. Simple pyridines form [N–F–N]⁺ halogen bonds with Selectfluor to facilitate single-electron reduction by catalytic Ag(I). Pyridine electronics affect the extent of halogen bonding, leading to significant differences in selectivity between mono- and difluorinated products. Electronic structure calculations show that halogen bonding to various pyridines alters the single-electron reduction potential of Selectfluor, which is consistent with experimental electrochemical analysis. Multinuclear correlation NMR also provides spectroscopic evidence for pyridine halogen bonding to Selectfluor under ambient conditions.

KEYWORDS: halogen-bonding, fluorination, H atom abstraction, HAT, radical



Noncovalent bonding interactions are broadly important to the field of organic chemistry. Electrostatic interactions including van der Waals forces, π – π stacking, ion– π interactions, and hydrogen bonding are all capable of modulating local electron density, resulting in altered physical or chemical properties.^{1–4} Hydrogen bonding in particular has been critical to the development of organocatalysis, where enhanced reactivity or asymmetric transformations may be promoted through hydrogen-bound intermediates.⁵ Great advances have been made over several decades, with the design and optimization of new catalysts being guided by experimental and theoretical evaluation of hydrogen bonding networks.⁶ Although a hydrogen bond acceptor may be any Lewis basic atom, the very nature of hydrogen bonding limits the hydrogen bond donor to the hydrogen atom. In contrast, electrostatic interactions between a Lewis basic atom and a halogen may provide intermediates of varying physical and chemical properties depending on the size and electronegativity of the halogen in question.⁷ Halogen bonding has gained attention as a potential surrogate for hydrogen bonding, and several recent reports demonstrate its utility in promoting organic transformations.⁸ Recently, halogen bonding between the fluorine of Selectfluor and electron-rich pyridines has been implicated in generating complexes that participate in single-electron transfer for heterobenzylic radical fluorinations (Scheme 1A).⁹ Our concurrent work in this area has suggested that a variety of electronically diverse pyridines interact with Selectfluor to affect Ag(I)-mediated single-electron reduction. We have found that the electronic characteristics of pyridine additives affect the

Scheme 1. Radical Fluorination via Halogen Bonding



efficiency of benzylic radical fluorination, and counterintuitive trends in product distribution are observed (Scheme 1B).

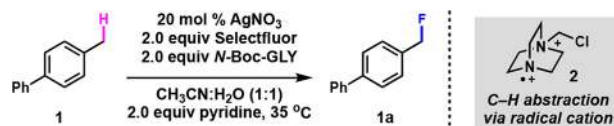
Received: February 11, 2019

Revised: March 8, 2019

Published: March 12, 2019

52 From our previous report on radical fluorination, we
53 concluded that amino acids acted as ligands to lower the
54 oxidation potential of Ag(I) to produce Ag(II) under mild
55 conditions.¹⁰ Binding Ag(I) through an electron-rich nitrogen
56 atom was critical to promote oxidation, with *N*-protected amino
57 acids failing to produce any observed reactivity. We
58 subsequently established that pyridine was a suitable ligand for
59 Ag(I), enabling C–H fluorination from previously ineffective *N*-
60 protected amino acids. Because a wide variety of pyridines are
61 readily available, we became interested in exploring them as
62 additives for our fluorination protocol. Control reactions with 4-
63 methylbiphenyl (**1**) showed that Ag(I), Selectfluor, and pyridine
64 were required for fluorination, but amino acid additives were not
65 (Table 1, entry 4). Reaction in the presence of (2,2,6,6-

Table 1. Discovery of Pyridine-Mediated Fluorination^a



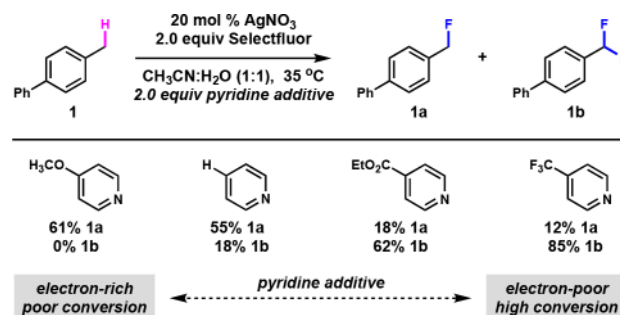
entry	deviation from standard conditions	Yield(%)
1	none	88
2	no AgNO ₃	00
3	no pyridine	00
4	no <i>N</i> -Boc-GLY	51
5	no <i>N</i> -Boc-GLY, TEMPO added	trace
6	<i>N</i> -fluoropyridinium instead of Selectfluor	00

^aNMR conversion versus 1,3,5-trimethoxybenzene. Standard conditions: 4-methylbiphenyl (**1**) (0.2 mmol), *N*-(*tert*-butoxycarbonyl)-glycine (*N*-Boc-GLY) (0.4 mmol), Selectfluor (0.4 mmol), AgNO₃ (0.04 mmol), pyridine (0.2 mmol), 2 mL CH₃CN:H₂O (1:1), 35 °C for 24 h.

66 tetramethylpiperidin-1-yl)oxyl (TEMPO) produced radical-
67 trapped adducts and inhibited fluorination (entry 5).¹¹ No
68 fluorinated products were observed using *N*-fluoropyridinium
69 tetrafluoroborate as a fluorine source (entry 6), suggesting that
70 fluorine transfer from Selectfluor to pyridine is not the source of
71 reactivity. On the basis of the mechanistic studies of Lectka, we
72 believed pyridine-mediated fluorination occurs via C–H
73 abstraction from the diazabicyclo radical cation **2** formed via
74 single-electron reduction of Selectfluor.¹² This mechanism relies
75 on Ag(I) only as an initiator and does not require a carboxylate
76 to reform Ag(I) via oxidative decarboxylation. In this
77 mechanism, **2** is presumably regenerated via radical fluorination
78 with Selectfluor to continue the radical chain process.

79 On the basis of these results, we explored a series of 4-
80 substituted pyridines as additives for radical fluorination. Our
81 original hypothesis was that pyridines served to lower the
82 oxidation potential of Ag(I), facilitating electron transfer. Cyclic
83 voltammetry showed that electron-rich pyridines produced
84 Ag(I) species with the lowest oxidation potentials, suggesting
85 facile single-electron transfer to Selectfluor from the electron-
86 rich metal. From these results, we expected a catalyst derived
87 from Ag(I) and 4-methoxypyridine to be optimum for
88 fluorination. However, we were surprised to find that electron-
89 rich pyridines were the *least* effective at promoting radical
90 fluorination of 4-methylbiphenyl (Scheme 2). Using two
91 equivalents of Selectfluor, a clear trend was observed whereby

Scheme 2. Pyridine-Dependent Product Distribution^a



^aNMR conversion versus 1,3,5-trimethoxybenzene. Conditions: 4-methylbiphenyl (**1**) (0.2 mmol), Selectfluor (0.4 mmol), AgNO₃ (0.04 mmol), pyridine (0.2 mmol), 2 mL CH₃CN:H₂O (1:1), 35 °C for 24 h.

electron-poor pyridines were the most efficient additives, 92
favoring difluorination as the major product. Experiments 93
using a 5-fold excess of Selectfluor show that difluorination is 94
possible from all pyridines examined. In situ ReactIR suggested 95
that pyridines interact directly with the [N–F]⁺ bond of 96
Selectfluor, leading us to consider the possibility of halogen 97
bonding as the source of our unexpected reactivity.¹¹ 98

Spectroscopic and theoretical work by Erdélyi established 99
pyridines as halogen bond acceptors, and his studies showed that 100
the extent of halogen bonding is affected by pyridine 101
electronics.¹³ In that work, diagnostic chemical shifts of pyridine 102
¹⁵N NMR signals were used to infer halogen bonding with *N*- 103
fluoropyridinium, but only minor changes in [N–¹⁹F]⁺ chemical 104
shift were observed under various conditions.¹⁴ Our own in situ 105
NMR studies under synthetic conditions yielded similar results, 106
with negligible shifts observed for the Selectfluor [N–¹⁹F]⁺ 107
signal in the presence of pyridine additives (Table 2). However, 108 12
we did observe significant changes in pyridine ¹⁵N chemical 109
shifts, as measured by ¹H/¹⁵N HMBC. In all cases examined, 110
pyridine ¹⁵N signals shifted to more negative values in the 111
presence of Selectfluor, consistent with the generation of a 112

Table 2. Chemical Shifts of Pyridines with Selectfluor[‡]

R	¹⁵ N	¹ H (C-2)	¹⁵ N	¹ H (C-2)	¹⁹ F
CF ₃	-67.31	7.95	-68.21	7.93	50.01
CO ₂ Et	-66.76	7.86	-70.54	7.86	50.03
H	-80.79	7.69	-92.64	7.66	50.01
OCH ₃	-102.59	7.51	-153.76 ^a	7.49	50.00
	-122.39	7.46	–	–	49.34

[‡]¹H and ¹⁵N chemical shifts referenced to nitromethane in a sealed capillary tube. ¹⁹F chemical shifts referenced to hexafluorobenzene in a sealed capillary tube. Conditions: pyridine (0.1 mmol), Selectfluor (0.1 mmol), in 700 uL of CD₃CN:H₂O (1:1) at 25 °C. ^aAveraged value of overlapping signals. Commercial *N*-fluoropyridinium tetrafluoroborate (0.1 mmol), in 700 uL of CD₃CN:H₂O (1:1) at 25 °C is provided as a reference.

113 “pyridinium-like” intermediate. Data for commercial *N*-
 114 fluoropyridinium is shown in Table 2 for comparison.
 115 In the case of 4-methoxypyridine, a shift of greater than 50 ppm
 116 is observed along the ^{15}N axis in the presence of Selectfluor,
 117 yielding a broad series of signals that coincides with line
 118 broadening of the C-2 ^1H NMR signal (Figure 1). In situ

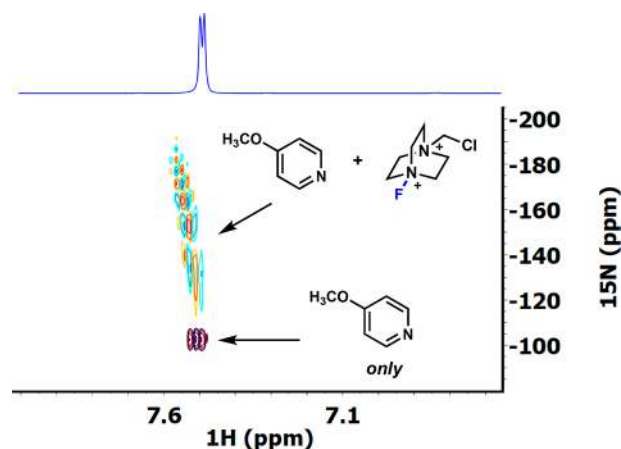


Figure 1. $^1\text{H}/^{15}\text{N}$ coupled HMBC of 4-methoxypyridine alone (maroon, blue) and with Selectfluor (yellow, teal, orange). Conditions: 4-methoxypyridine (0.1 mmol), Selectfluor (0.1 mmol), in 700 μL $\text{CD}_3\text{CN}/\text{D}_2\text{O}$ (1:1) at 25 $^\circ\text{C}$.

119 ReactIR shows that 4-methoxypyridine consumes Selectfluor
 120 under synthetic conditions without Ag(I) present, presumably
 121 either via nucleophilic displacement of fluorine or single-
 122 electron transfer as proposed by Van Humbeck.⁹ Similar effects
 123 are observed for pyridine, albeit with a smaller ^{15}N chemical shift
 124 and reduced rate of Selectfluor consumption. Interestingly,
 125 electron-poor pyridines do not consume Selectfluor in the
 126 absence of Ag(I), but exhibit clear interactions as evidenced by
 127 ^{15}N NMR and IR spectroscopy.¹¹ To further investigate the
 128 effects of halogen bonding on the efficiency of our radical
 129 fluorinations, we pursued computational evaluation of $[\text{N}-\text{F}-$
 130 $\text{N}]^+$ halogen bound intermediates involving pyridines and
 131 Selectfluor.

132 Computational efforts first involved determining the speci-
 133 ation and chemical properties of Ag(I)/pyridine complexes.
 134 Calculations using the B3PW91/6-311G(d) model chemistry
 135 including implicit solvation by acetonitrile were carried out
 136 using a local development version of Gaussian.^{15,16} The
 137 calculated Ag(I) oxidation potentials showed that bis-pyridine
 138 Ag(I) species are the most likely reductants to initiate radical
 139 fluorination.¹¹ Calculated E^0 values for a series of bis-pyridine
 140 Ag(I) adducts were consistent with experimental values
 141 measured directly via cyclic voltammetry, confirming that
 142 electron-rich pyridines lead to easily oxidized Ag(I) initiators.

143 With experimental and theoretical results in agreement
 144 regarding Ag(I) oxidation, we turned to modeling halogen-
 145 bound pyridine/Selectfluor complexes. Preliminary results
 146 suggested density functional theory (DFT) model chemistries,
 147 including those with empirical dispersion corrections are unable
 148 to treat the physics of the $[\text{N}-\text{F}-\text{N}]^+$ halogen bond. Noting two
 149 extensive benchmark reports by Martin and by Wong,¹⁷
 150 indicating only a limited set of approximate functionals are
 151 capable of predicting halogen bonding strengths, we suspect our
 152 observations are due to the exceptionally electron-deficient
 153 character of the $[\text{N}-\text{F}-\text{N}]^+$ motif. Therefore, we turned to

correlated wave function methods. Geometries of candidate
 154 halogen-bound species were optimized with the MP2/6-
 155 311+G(d) level of theory and single-point energies were
 156 evaluated with the CCSD(T)/6-311+G(d) model chemistry
 157 including implicit solvation. These calculations identified
 158 pyridine/Selectfluor complexes featuring the anticipated $[\text{N}-$
 159 $\text{F}-\text{N}]^+$ bonding motif (Table 3, eq 1). The halogen-bound
 160 161

Table 3. Trends for Selectfluor-Pyridine Halogen Bond

R group	$\Delta H1$ (kcal/mol)	$\Delta H2$ (kcal/mol)
OCH ₃	0.34	-31.42
H	0.74	-31.82
CO ₂ Et	3.63	-33.66
CF ₃	2.57	-34.71

species are slightly higher in energy (<1–4 kcal/mol) than the
 162 unbound species, though subsequent reduction to form
 163 diazabicyclo radical cation 2 is quite favorable (Table 3, eq 2,
 164 vide infra).

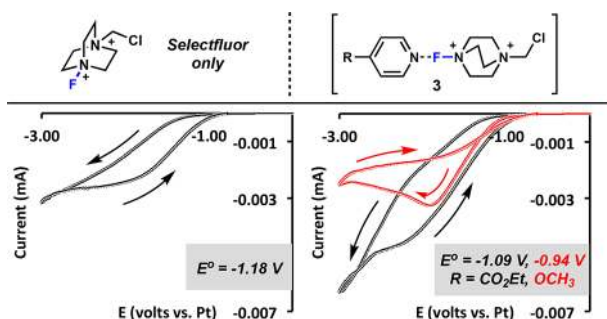
Computational results suggested that electron-rich pyridines
 165 were more effective halogen bond acceptors than electron-
 166 deficient pyridines, which agreed with chemical shift data
 167 provide in Table 2.¹⁸ As shown in Table 3, the energetics of $[\text{N}-$
 168 $\text{F}-\text{N}]^+$ bond reduction via single-electron transfer exhibit a clear
 169 trend depending on the electronic characteristics of the pyridine.
 170 Interestingly, all structures exhibit similar bond lengths for both
 171 N–F bonds (~ 1.84 Å) in the complex and a linear N–F–N
 172 bond angle. We were pleased to note that the reduction of the
 173 $[\text{N}-\text{F}-\text{N}]^+$ halogen-bound complex is most energetically
 174 favorable with an electron-poor pyridine. These data correlate
 175 directly to the experimental reactivity trends observed in
 176 Scheme 2, whereby electron-poor pyridines are the most
 177 efficient at promoting radical fluorination. Studies exploring
 178 alternative bonding interactions, including halogen bonding to
 179 the chlorine of Selectfluor, showed the only suitable geometry is
 180 as shown in structure 3. In addition, because synthetic
 181 experimental conditions include water as a cosolvent, the
 182 possibility of a mixed hydrogen/halogen bonding network was
 183 also explored computationally.¹¹ The inclusion of discrete water
 184 molecules into complex 3 did not converge into meaningful
 185 structures, suggesting the effects reported in Table 2 are the
 186 result of direct interaction between the pyridine nitrogen and
 187 Selectfluor $[\text{N}-\text{F}]^+$.

Exploring the extent to which post-SCF correlation affects the
 189 electron density to give rise to the $[\text{N}-\text{F}-\text{N}]^+$ weak interaction,
 190 we evaluated the difference between MP2 and reference
 191 Hartree–Fock electron densities. Scheme 1B shows such a
 192 depiction for 3. Electron correlation yields symmetric
 193 redistribution of electron density in the two N–F bonding
 194 regions, which is consistent with our analysis that post-SCF
 195 treatment is required to properly account for the $[\text{N}-\text{F}-\text{N}]^+$
 196 weak interactions.

To further explore the effects of pyridine/Selectfluor
 198 interactions in the context of radical initiation, we examined
 199 the electrochemical reduction of Selectfluor under synthetic
 200 201

201 conditions. As shown in Scheme 3, Selectfluor produces an
202 irreversible single-electron reduction at approximately -1.18 V.

Scheme 3. Electrochemical Reduction of Selectfluor^a

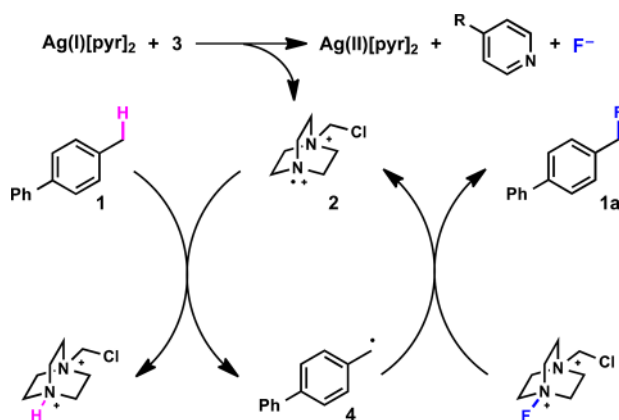


^aConditions: Selectfluor (0.5 mmol) in 5 mL of CH₃CN:H₂O (1:1), tetrabutylammonium tetrafluoroborate supporting electrolyte (0.1 M), pyridine (where applicable) (0.5 mmol). Left: Selectfluor alone (black curve). Right: Selectfluor with ethyl isonicotinate (black curve), and 4-methoxypyridine (red curve). Arrows indicate the direction of applied potential. E⁰ values are determined as the minimum voltage producing $-100 \mu\text{A}$ of current in the reducing direction.

203 This value was clearly perturbed by the presence of pyridine
204 additives to yield species that reduce at lower potentials than
205 Selectfluor alone, consistent with the energies calculated for
206 ΔH_2 in Table 3 above.

207 On the basis of our combined experimental and computa-
208 tional results, we propose the following mechanism for radical
209 C–H fluorination with Selectfluor via Ag(I)/pyridine initiators
210 (Scheme 4). Analytical electrochemistry and computations

Scheme 4. Proposed Mechanism



211 demonstrate that Ag(I)/pyridine complexes are better reduc-
212 tants than Ag(I) alone, suggesting a pre-equilibrium to bis-
213 pyridine Ag(I) complexes. Single-electron transfer to a halogen-
214 bound pyridine/Selectfluor complex 3 would produce Ag(II)-
215 [pyr]₂, pyridine, fluoride anion, and diazabicyclo radical cation
216 2. C–H abstraction of 1 produces nucleophilic radical 4 that
217 quenches with an additional equivalent of Selectfluor to
218 regenerate 2, propagating the radical reaction. At this stage of
219 investigation, it is unclear whether halogen-bonding is required
220 for Selectfluor reduction, or if all Ag(I)[pyr]₂ initiators
221 investigated are sufficiently reducing to produce 2. One
222 contributing factor to the marked difference in efficiency
223 shown in Scheme 2 is unproductive consumption of Selectfluor

from electron-rich pyridines. However, it cannot be the only
224 factor affecting reaction efficiency, as the trend correlating
225 pyridine electronics to efficiency holds for pyridines that do not
226 affect the concentration of Selectfluor in an unproductive
227 manner.

In conclusion, we have demonstrated experimental and
229 theoretical evidence supporting the presence of halogen
230 bonding in pyridine-mediated radical fluorinations. Two-
231 dimensional NMR shows clear ¹⁵N shifts of pyridine additives
232 when exposed to Selectfluor under synthetic conditions. 233
Counterintuitive trends in reaction efficiency are rationalized
234 via computational modeling of [N–F–N]⁺ intermediates and in
235 situ reaction monitoring, leading to a clearer picture of electron
236 transfer between Ag(I)[pyr]₂ initiators and Selectfluor in the
237 presence of pyridine. Analytical electrochemistry shows that
238 pyridine additives affect the single-electron reduction of
239 Selectfluor, consistently producing species that are more easily
240 reduced. A comprehensive mechanistic picture of radical
241 fluorination likely involves equilibration of pyridine with both
242 Ag(I) and Selectfluor, leading to a complicated kinetic scenario
243 that we are currently studying via in situ reaction monitoring and
244 computational modeling. 245

ASSOCIATED CONTENT

Supporting Information

The Supporting Information is available free of charge on the
ACS Publications website at DOI: 10.1021/acscatal.9b00623.

Computational procedures, optimized geometries, and
the full Gaussian citation (PDF)

General considerations and reaction procedures and
supplemental data (PDF)

AUTHOR INFORMATION

Corresponding Authors

*E-mail: hhratchian@ucmerced.edu.

*E-mail: rbaxter@ucmerced.edu.

ORCID

Hrant P. Hrachian: 0000-0003-1436-5257

Ryan D. Baxter: 0000-0002-1341-5315

Author Contributions

†(A.M.H., S.L.B.) These authors contributed equally to this
work.

Notes

The authors declare no competing financial interest.

ACKNOWLEDGMENTS

S.L.B. acknowledges the faculty mentor fellowship program at
UC Merced. H.P.H. acknowledges the ACS-PRF No. S6806-
DNI6, computing time on the MERCED cluster supported by
the National Science Foundation under Grant No. ACI-
1429783, and the Hellman Fellows Fund for a faculty fellowship.
R.D.B. acknowledges the ACS-PRF No. S6225-DNIS. This
material is based upon work supported by the National Science
Foundation under Grant No. 1752821 (R.D.B.). We thank Dave
Rice for his help in the acquisition and interpretation of NMR
spectra.

REFERENCES

(1) Parsegian, V. A. *Van der Waals Forces: A Handbook for Biologists, Chemists, Engineers, and Physicists*; Cambridge University Press: 279
Cambridge and New York, 2006; pp 41–98. 280

- 281 (2) (a) Hunter, C. A.; Sanders, J. K. M. The Nature of π - π
282 Interactions. *J. Am. Chem. Soc.* **1990**, *112*, 5525–5534. (b) Neel, A. J.;
283 Hilton, M. J.; Sigman, M. S.; Toste, F. D. Exploiting Non-Covalent π
284 Interactions for Catalyst Design. *Nature* **2017**, *543*, 637–646.
- 285 (3) (a) Frontera, A.; Gamez, P.; Mascal, M.; Mooibroek, T. J.; Reedijk,
286 J. Putting Anion- π Interactions into Perspective. *Angew. Chem., Int. Ed.*
287 **2011**, *50*, 9564–9583. (b) Mahadevi, A. S.; Sastry, G. N. Cation- π
288 Interaction: Its Role and Relevance in Chemistry, Biology, and Material
289 Science. *Chem. Rev.* **2013**, *113*, 2100–2138.
- 290 (4) (a) Jeffrey, G. A. *An Introduction to Hydrogen Bonding*; Oxford
291 University Press: New York, 1997, Vol. 4, p 303. (b) Grabowski, S.
292 *Chem. Rev.* **2011**, *111*, 2597–2625.
- 293 (5) Doyle, A. G.; Jacobsen, E. N. Small-Molecule H-Bond Donors in
294 Asymmetric Catalysis. *Chem. Rev.* **2007**, *107*, 5713–5743.
- 295 (6) (a) Hamza, A.; Schubert, G.; Soos, T.; Papai, I. Theoretical Studies
296 on the Bifunctionality of Chiral Thiourea-Based Organocatalysts:
297 Competing Routes to C–C Bond Formation. *J. Am. Chem. Soc.* **2006**,
298 *128*, 13151–13160. (b) Armstrong, A.; Boto, R. A.; Dingwall, P.;
299 Contreras-Garcia, J.; Harvey, M. J.; Mason, N. J.; Rzepa, H. S. The
300 Houk-List Transition States for Organocatalytic Mechanisms Revisited.
301 *Chem. Sci.* **2014**, *5*, 2057–2071. (c) Zabka, M.; Sebesta, R.
302 Experimental and Theoretical Studies of Hydrogen-Bonding in
303 Organocatalysis. *Molecules* **2015**, *20*, 15500–15524. (d) Grayson, M.
304 N. Mechanism and Origins of Stereoselectivity in the Cinchona
305 Thiourea- and Squaramide-Catalyzed Asymmetric Michael Addition of
306 Nitroalkanes to Enones. *J. Org. Chem.* **2017**, *82*, 4396–4401.
- 307 (7) Desiraju, G. R.; Ho, P. S.; Kloo, L.; Legon, A. C.; Marquardt, R.;
308 Metrangolo, P.; Politzer, P.; Resnati, G.; Rissanen, K. Definition of the
309 halogen bond (IUPAC Recommendations 2013). *Pure Appl. Chem.*
310 **2013**, *85*, 1711–1713.
- 311 (8) (a) Nagorny, P.; Sun, Z. New approaches to organocatalysis based
312 on C–H and C–X bonding for electrophilic substrate activation.
313 *Beilstein J. Org. Chem.* **2016**, *12*, 2834–2848. (b) Guha, S.; Kazi, I.;
314 Nandy, A.; Sekar, G. Role of Lewis-Base-Coordinated Halogen(I)
315 Intermediates in Organic Synthesis: The Journey from Unstable
316 Intermediates to Versatile Reagents. *Eur. J. Org. Chem.* **2017**, *2017*,
317 5497–5518. (c) Chen, M.-W.; Ji, Y.; Wang, J.; Chen, Q.-A.; Shi, L.;
318 Zhou, Y.-G. Asymmetric Hydrogenation of Isoquinolines and Pyridines
319 Using Hydrogen Halide Generated in Situ as Activator. *Org. Lett.* **2017**,
320 *19*, 4988–4991. (d) Ma, R.; He, L.-N.; Liu, X.-F.; Liu, X.; Wang, M.-Y.
321 DBU as Activator for the *N*-iodosuccinimide Promoted Chemical
322 Fixation of Carbon Dioxide with Epoxides. *Journal of CO₂ Utilization*
323 **2017**, *19*, 28–32. (e) Kobayashi, Y.; Nakatsuji, Y.; Li, S.; Tsuzuki, S.;
324 Takemoto, Y. Direct *N*-Glycofunctionalization of Amides with Glycosyl
325 Trichloroacetimidate by Thiourea/Halogen Bond Donor Co-Catalysis.
326 *Angew. Chem., Int. Ed.* **2018**, *57*, 3646–3650. (f) Lu, Y.; Nakatsuji, H.;
327 Okumura, Y.; Yao, L.; Ishihara, K. Enantioselective Halo-oxy- and
328 Halo-azacyclizations Induced by Chiral Amidophosphate Catalysts and
329 Halo-Lewis Acids. *J. Am. Chem. Soc.* **2018**, *140*, 6039–6043.
- 330 (g) Brückner, R.; Haller, H.; Steinhauer, S.; Müller, C.; Riedel, S. A
331 2D Polychloride Network Held Together by Halogen-Halogen
332 Interactions. *Angew. Chem., Int. Ed.* **2015**, *54*, 15579–15583. (h) Riedel,
333 S.; Köchner, T.; Wang, X.; Andrews, L. Polyfluoride Anions, a Matrix-
334 Isolation and Quantum-Chemical Investigation. *Inorg. Chem.* **2010**, *49*,
335 7156–7164. (i) Gliese, J.; Jungbauer, S. H.; Huber, S. M. A Halogen-
336 Bonding-Catalyzed Michael Addition Reaction. *Chem. Commun.* **2017**,
337 *53*, 12052–12055. (j) Heinen, F.; Engelage, E.; Dreger, A.; Weiss, R.;
338 Huber, S. M. Iodine(III) Derivatives as Halogen Bonding Organo-
339 catalysts. *Angew. Chem., Int. Ed.* **2018**, *57*, 3830–3833. (k) Schindler, S.;
340 Huber, S. M. Halogen Bonds in Organic Synthesis and Organocatalysis.
341 In *Halogen Bonding II: Impact on Materials Chemistry and Life Sciences*;
342 Metrangolo, P., Resnati, G., Eds.; Springer International Publishing:
343 Cham, 2015; Vol. 359, pp 167–204. (l) Breugst, M.; von der Heiden, D.
344 Mechanisms in Iodine Catalysis. *Chem. - Eur. J.* **2018**, *24*, 9187. (m) von
345 der Heiden, D.; Detmar, E.; Kuchta, R.; Breugst, M. Activation of
346 Michael Acceptors by Halogen-Bond Donors. *Synlett* **2018**, *29*, 1307–
347 1313. (n) Breugst, M.; von der Heiden, D.; Schmauck, J. Novel
348 Noncovalent Interactions in Catalysis: A Focus on Halogen,
349 Chalcogen, and Anion- π Bonding. *Synthesis* **2017**, *49*, 3224–3236.
- (9) Danahy, K. E.; Cooper, J. C.; Van Humbeck, J. F. Benzylic
350 Fluorination of Aza-Heterocycles Induced by Single-Electron Transfer
351 to Selectfluor. *Angew. Chem., Int. Ed.* **2018**, *57*, 5134–5138.
- (10) Hua, A. M.; Mai, D. N.; Martinez, R.; Baxter, R. D. Radical C–H
353 Fluorination Using Unprotected Amino Acids as Radical Precursors.
354 *Org. Lett.* **2017**, *19*, 2949–2952.
- (11) See Supporting Information for further details. 355
- (12) (a) Pitts, C. R.; Bloom, S.; Woltornist, R.; Auvenshine, D. J.;
357 Ryzhkov, L. R.; Siegler, M. A.; Lectka, T. Direct, Catalytic
358 Monofluorination of sp^3 C–H Bonds: A Radical-Based Mechanism
359 with Ionic Selectivity. *J. Am. Chem. Soc.* **2014**, *136*, 9780–9791. 360
(b) Pitts, C. R.; Ling, B.; Woltornist, R.; Liu, R.; Lectka, T.
361 Triethylborane-Initiated Radical Chain Fluorination: A Synthetic
362 Method Derived from Mechanistic Insight. *J. Org. Chem.* **2014**, *79*,
363 8895–8899. 364
- (13) (a) Carlsson, A.-C. C.; Veiga, A. X.; Erdélyi, M. Halogen Bonding
365 in Solution. In *Halogen Bonding II: Impact on Materials Chemistry and*
366 *Life Sciences*; Metrangolo, P., Resnati, G., Eds.; Springer International
367 Publishing: Cham, 2015; Vol. 359, pp 49–76. (b) Bedin, M.; Karim, A.;
368 Reitti, M.; Carlsson, A.-C. C.; Topic, F.; Cetina, M.; Pan, F.; Havel, V.;
369 Al-Ameri, F.; Sindelar, V.; Rissanen, K.; Grafenstein, J.; Erdelyi, M.
370 Counterion Influence on the N–I–N Halogen Bond. *Chem. Sci.* **2015**,
371 *6*, 3746–3756. (c) Carlsson, A.-C. C.; Mehmeti, K.; Uhrbom, M.;
372 Karim, A.; Bedin, M.; Puttreddy, R.; Kleinmaier, R.; Neverov, A. A.;
373 Nekoueiashahraki, B.; Gräfenstein, J.; Rissanen, K.; Erdélyi, M.
374 Substituent Effects on the $[N-I-N]^+$ Halogen Bond. *J. Am. Chem.*
375 *Soc.* **2016**, *138*, 9853–9863. 376
- (14) Karim, A.; Reitti, M.; Carlsson, A.-C. C.; Grafenstein, J.; Erdelyi,
377 M. The Nature of $[N-Cl-N]^+$ and $[N-F-N]^+$ Halogen Bonds in
378 Solution. *Chem. Sci.* **2014**, *5*, 3226–3233. 379
- (15) Frisch, M. J.; Trucks, G. W.; Schlegel, H. B.; Scuseria, G. E.;
380 Robb, M. A.; Cheeseman, J. R.; Scalmani, G.; Barone, V.; Petersson, G.
381 A.; Nakatsuji, H.; Li, X.; Caricato, M.; Marenich, A. V.; Bloino, J.;
382 Janesko, B. G.; Gomperts, R.; Mennucci, B.; Hratchian, H. P.; Ortiz, J.
383 V.; Izmaylov, A. F.; Sonnenberg, J. L.; Williams-Young, D.; Ding, F.;
384 Lipparini, F.; Egidi, F.; Goings, J.; Peng, B.; Petrone, A.; Henderson, T.;
385 Ranasinghe, D.; Zakrzewski, V. G.; Gao, J.; Rega, N.; Zheng, G.; Liang,
386 W.; Hada, M.; Ehara, M.; Toyota, K.; Fukuda, R.; Hasegawa, J.; Ishida,
387 M.; Nakajima, T.; Honda, Y.; Kitao, O.; Nakai, H.; Vreven, T.;
388 Throssell, K.; Montgomery, J. A., Jr.; Peralta, J. E.; Ogliaro, F.; Bearpark,
389 M. J.; Heyd, J. J.; Brothers, E. N.; Kudin, K. N.; Staroverov, V. N.; Keith,
390 R.; Kobayashi, J.; Normand, K.; Raghavachari, A. P.; Rendell, J. C.;
391 Burant, S. S.; Iyengar, J.; Tomasi, M.; Cossi, J. M.; Millam, T. A.; Klene,
392 M.; Adamo, C.; Cammi, R.; Ochterski, J. W.; Martin, R. L.; Morokuma,
393 K.; Farkas, O.; Foresman, J. B.; Fox, D. J.; *Gaussian*, Development
394 Version, Revision I.10+; Gaussian, Inc.: Wallingford, CT, 2016. 395
- (16) (a) Becke, A. D. Density-functional thermochemistry. III. The
396 role of exact exchange. *J. Chem. Phys.* **1993**, *98*, 5648. (b) Wang, Y.;
397 Perdew, J. P. Spin scaling of the electron-gas correlation energy in the
398 high-density limit. *Phys. Rev. B: Condens. Matter Mater. Phys.* **1991**, *43*,
399 8911. 400
- (17) (a) Kozuch, S.; Martin, J. M. L. Halogen Bonds: Benchmarks and
401 Theoretical Analysis. *J. Chem. Theory Comput.* **2013**, *9*, 1918–1931. 402
(b) Anderson, L. N.; Aquino, F. W.; Raeber, A. E.; Chen, X.; Wong, B.
403 M. Halogen Bonding Interactions: Revised Benchmarks and a New
404 Assessment of Exchange vs Dispersion. *J. Chem. Theory Comput.* **2018**,
405 *14*, 180–190. 406
- (18) Correlation of computed binding constants to $^1\text{H-NMR}$
407 chemical shifts was attempted using the web-based software at [www.
408 app.supramolecular.org/bindfit/](http://www.app.supramolecular.org/bindfit/). These results are provided in the
409 Supporting Information. 410